chemosensors

MDPI

Article

3D-Printed Graphene Electrodes Applied in an Impedimetric Electronic Tongue for Soil Analysis

Tatiana Americo da Silva [1], Maria Luisa Braunger [1], Marcos Antonio Neris Coutinho [2], Lucas Rios do Amaral [2], Varlei Rodrigues [1] and Antonio Riul Jr. [1,*]

[1] Department of Applied Physics, "Gleb Wataghin" Institute of Physics, University of Campinas—UNICAMP, Campinas 13083-859, SP, Brazil; tati.americo@hotmail.com (T.A.d.S.); malubraunger@yahoo.com.br (M.L.B.); varlei@ifi.unicamp.br (V.R.)

[2] School of Agricultural Engineering, University of Campinas—UNICAMP, Campinas 13083-875, SP, Brazil; marcos_eafsal@hotmail.com (M.A.N.C.); lucas.amaral@feagri.unicamp.br (L.R.d.A.)

* Correspondence: riul@ifi.unicamp.br

Received: 17 September 2019; Accepted: 22 October 2019; Published: 24 October 2019

Abstract: The increasing world population leads to the growing demand for food production without expanding cultivation areas. In this sense, precision agriculture optimizes the production and input usage by employing sensors to locally monitor plant nutrient within agricultural fields. Here, we have used an electronic tongue sensing device based on impedance spectroscopy to recognize distinct soil samples (sandy and clayey) enriched with macronutrients. The e-tongue setup consisted of an array of four sensing units formed by layer-by-layer (LbL) films deposited onto 3D-printed graphene-based interdigitated electrodes (IDEs). The IDEs were fabricated in 20 min using the fused deposition modeling process and commercial polylactic acid-based graphene filaments. The e-tongue comprised one bare and three IDEs functionalized with poly(diallyldimethylammonium chloride) solution/copper phthalocyanine-3,4′,4″,4‴-tetrasulfonic acid tetrasodium salt (PDDA/CuTsPc), PDDA/montmorillonite clay (MMt-K), and PDDA/poly(3,4-ethylenedioxythiophene)-poly(styrenesulfonate) (PEDOT:PSS) LbL films. Control samples of sandy and clayey soils were enriched with different concentrations of nitrogen (N), phosphorus (P), and potassium (K) macronutrients. Sixteen soil samples were simply diluted in water and measured using electrical impedance spectroscopy, with data analyzed by principal component analysis. All soil samples were easily distinguished without pre-treatment, indicating the suitability of 3D-printed electrodes in e-tongue analysis to distinguish the chemical fertility of soil samples. Our results encourage further investigations into the development of new tools to support precision agriculture.

Keywords: layer-by-layer films; e-tongue; soil analysis; 3D printing

1. Introduction

A crucial problem nowadays is the need to increase food production without expanding agricultural areas [1]. Within this context, precision agriculture explores the development of sensors to locally monitor the level of plant nutrients available in the soil, aimed at variable-rate fertilizer application [2,3]. Traditional soil chemical analysis is usually time-consuming and expensive [4], which leads to soil sampling density below that required to properly map the spatial variability of soil fertility [5,6], motivating the development of alternative approaches for sensing in agricultural practices [7].

Electronic tongue devices are interesting alternative tools to address existing challenges [8]. Briefly, an e-tongue is a multisensory system employed in the analysis of complex liquid media that transforms raw data into specific recognition patterns that are further visualized through computational and statistical analysis [9–11]. There is a myriad of applications in the literature including not only

edible foodstuff [12] and beverages [13–16] but also in non-edible analytes, such as environmental pollutants [17–19], pesticides [20,21], elements of medical concern [22–24], and soil [25,26].

There are only a few papers in the literature combining e-tongue systems and soil analysis. Mimendia et al. proposed an array of 20 ion-selective electrodes for potentiometric measurements and artificial neural networks (ANNs) for pattern recognition in soil analysis [25]. The authors were able to distinguish six distinct soil types based on their extract components in distilled water, barium chloride, and acetic acid. In addition, a quantitative response model to directly estimate organic carbon content, K^+, Mg^{2+}, NO_3^-, and Cl^- was developed from a properly trained ANN, presenting satisfactory results when compared to traditional methods. Braunger et al. proposed a microfluidic e-tongue based on layer-by-layer (LbL) thin films and electrical impedance spectroscopy to qualitative discriminate soil samples enriched with N, P, K, Ca, Mg, and S [26] that were simply diluted in water and analyzed under flow conditions. The capacitance data were dimensionally reduced by principal component analysis (PCA), interactive document map (IDMAP), and Sammon's mapping to facilitate data visualization for comparison.

E-tongue systems require electrode fabrication, and that usually requires photolithography and microfabrication processes, thus enabling the fabrication of specific geometries in the micrometer range. Such techniques demand multistep processing, specialized facilities, trained personnel, and the use of toxic and expensive reagents. However, in the last decade, inkjet and 3D printing technologies have emerged as alternative methods for simpler fabrication of electrodes using non-conventional conductive materials [27,28]. 3D printing has attracted great attention due to the capacity for customization and rapid prototyping, consuming fewer resources, and generating fewer residues than traditional techniques. For sensor development, 3D printing is a promising additive manufacturing technology as it allows easy changes in electrode features, fabrication of small parts or molds designed for a specific application in customized geometries, and also to print accessories to fit or integrate with commercial electronic devices [29].

In this manuscript, we integrate the emergent 3D printing technology to fabricate an e-tongue system, using LbL films as sensing units and electrical impedance spectroscopy in the analysis of sandy and clayey soil samples enriched with distinct amounts of nitrogen (N), phosphorus (P), and potassium (K). The aim here is to find an alternative, robust approach for a faster fabrication of e-tongue systems applied in soil analysis. The results were promising compared to our previous work using gold electrodes, as there was no loss of information in the samples' identification, highlighting 3D printing technology as a valuable tool for faster prototyping of e-tongue systems.

There are different types of commercial sensors for soil analysis. However, none of them integrate 3D printing and e-tongue analysis, which is the primary idea of the study presented here. The research conducted in our research group so far has led us to believe that it is possible to use e-tongue systems based on LbL films and impedance measurements to evaluate soil samples by simply diluting them in water. Here, we are taking the first step towards showing that beyond discriminant analysis of the soil samples, it is possible to correlate electric signals and macronutrients at distinct concentrations using a simplified e-tongue system. There is a long road from this point to the development of a commercial sensor, but the results presented here are point to the feasibility of such sensors. In case of future success, some advantages to this system are fast and simple prototyping, use of biodegradable materials, and small amounts for sampling and discard. Additionally, it allows the construction of inexpensive equipment for on-site measurements based on basic commercial electronics.

2. Materials and Methods

2.1. Electrodes Fabrication

Interdigitated electrodes (IDEs) were fabricated with a conductive filament and the fused deposition modeling (FDM) method using a homemade two nozzle CoreXY FDM 3D printer built based on the RepRap open hardware, as previously reported [30]. The conductive filament was a

commercial polylactic acid (PLA)-based thermoplastic doped with graphene fibers purchased from BlackMagic 3D (Graphene Supermarket, Ronkonkoma, NY, USA). Planar IDEs were designed with 3 pairs of digits having 9 mm length, 1 mm width, and digits spaced 1 mm from each other. The IDEs were printed in 20 min (on average), while the photolithography process to fabricate gold IDEs usually takes a couple of hours.

2.2. Layer-by-Layer Films

Copper phthalocyanine-3,4′,4″,4‴-tetrasulfonic acid tetrasodium salt (CuTsPc), montmorillonite clay (MMt-K), poly (3,4-ethylenedioxythiophene)-poly (styrenesulfonate) (PEDOT:PSS), and poly (diallyldimethylammonium chloride) solution (PDDA) were purchased from Sigma–Aldrich and used as received. All materials were dispersed in ultrapure water acquired from an Arium comfort Sartorius system.

The LbL technique was chosen due to its simplicity to promote surface modification at the nanoscale using intermolecular non-covalent interactions of oppositely charged polyelectrolytes. Briefly, the LbL technique consists of immersing a solid substrate in an aqueous solution containing the material to be adsorbed. Subsequently, the substrate is rinsed to remove material that is loosely bound, allowed to dry, and then immersed in another polyelectrolyte solution having the opposite charge to the material initially adsorbed [31]. Then, multilayered thin films are formed by alternating adsorbed cationic and anionic molecular bilayers.

Since each sensing unit had 50 bilayers deposited onto the IDEs and the average thickness of a deposited layer in an LbL film was ~2 nm, the LbL film thickness was ~100 nm.

2.3. Soil Samples

Two soils of different textures (clayey and sandy) with low natural fertility were collected in Campinas (SP/Brazil) [32] and classified here as control samples (S-000). They were both enriched with different amounts of N, P, and K, resulting in soil samples codified as S-100, S-010, S-001, S-200, S-020, S-002, S-222. The numeric sequence is related to the NPK addition of macronutrients in each sample and S (from sample) was added to avoid confusion with numerical quantities throughout the manuscript. The content levels that were effectively obtained are presented in Table 1. In this sample code, 0 represents the lowest concentration (natural fertility), 1 refers to medium concentration, and 2 is related to higher concentrations of macronutrients.

Table 1. Sandy and clayey soils composition regarding N, P, and K availability, according to traditional soil chemical analysis. The units of measurement are $g \cdot kg^{-1}$, $mg \cdot dm^{-3,}$ and $mmol_c \cdot dm^{-3}$ for N, P, and K, respectively.

Sample Code (S-NPK)	Sandy Soil	Clayey Soil
S-000	406, 6, 0.9	945, 1, 0.5
S-100	378, 6, 1	994, 12, 0.6
S-010	406, 21, 0.9	917, 220, 0.7
S-001	462, 4, 4.7	924, 1, 4
S-200	379, 6, 0.9	994, 15, 0.4
S-020	364, 314, 0.9	973, 419, 1
S-002	378, 4, 16	910, 1, 8.4
S-222	371, 126, 11.7	1057, 464, 7.3

2.4. E-tongue Analysis

The idea in an e-tongue system is to mimic the biological system. Taste buds in the human tongue, when in contact with foodstuffs, send electrical stimulus to the brain, which has the unique capability of grouping them all into specific patterns that are classified in tastes. In analogy, an array of sensing units based on electrodes functionalized with materials having distinct chemical compositions create a

"fingerprint" of the sample through different electroanalytical responses. Then, the information can be processed using statistical and computational techniques to identify a sample analyte.

The e-tongue system presented here was composed of one bare electrode and three IDEs covered with PDDA/CuTsPc, PDDA/MMt-K, and PDDA/PEDOT:PSS LbL films, similar to [26,30]. Electrical measurements were performed using 25 mV of amplitude in the frequency range 1–10^6 Hz using a Solartron 1260A impedance/gain-phase analyzer coupled to a 1296A dielectric interface. For the e-tongue analysis, all soil samples were prepared at 1 mg·mL^{-1} in ultrapure water, followed by 30 min of sonication. The electrical measurements were performed for all soil samples in solution at each sensing unit dipped under constant and non-turbulent stirring to avoid soil decantation. All 16 soil samples (8 sandy and 8 clayey soils) were measured using the 4 sensing units in triplicate, resulting in 192 independent measurements. Figure 1 presents the experimental setup for the e-tongue system applied in the soil analyses. It is worth mentioning additional measurements taken in distilled water before and after each soil sample were analyzed to check possible cross-contamination along with data acquisition as well.

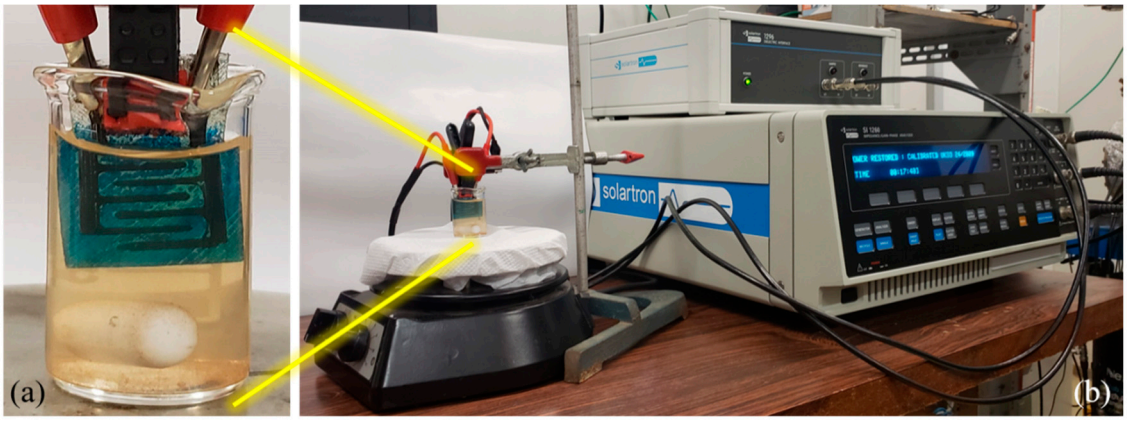

Figure 1. (**a**) Zoom at one of the sensing units (poly(diallyldimethylammonium chloride) solution/copper phthalocyanine-3,4′,4″,4‴-tetrasulfonic acid tetrasodium salt (PDDA/CuTsPc)) in the beaker with a soil sample in aqueous solution and (**b**) experimental setup used for the e-tongue analysis with electrical measurements.

After acquisition, the capacitance data were dimensionally reduced by principal component analysis (PCA). PCA is a statistical method widely used in pattern recognition to reduce the dimensionality of the raw data, thus facilitating information visualization. This method consists of rewriting the coordinates of a data set (input matrix) into a new orthogonal axis system called principal components. New coordinates (scores) are from the linear combination of the original variables so that the data can be represented by a smaller number of descriptive factors, reducing the size of the analyzed set with minimal loss or redundancy of information. Here, we have used the real part of the capacitance, *C*, and the PCA plots were obtained from *C* at a fixed frequency (1 kHz) for each of the sensing units.

2.5. Limit of Detection

The limit of detection (LOD) of two sensing units (bare IDEs and PDDA/PEDOT:PSS) were calculated for two soil samples (S-000 and S-002). Electrical measurements were performed in the soil samples diluted in distinct concentrations from 0.1 to 1 mg·mL^{-1}.

3. Results and Discussion

Impedance spectra were obtained for the four sensing units (bare, PDDA/CuTsPc, PDDA/MMt-K, and PDDA/PEDOT:PSS onto 3D-printed IDEs) in distilled water (Figure 2). The impedance results

were similar to those obtained for the same LbL films deposited on gold IDEs previously reported [26]. The observed differences in the electrical responses of the sensing units immersed in distilled water are probably related to the insulating nature of montmorillonite clays [33] since CuTsPc and PEDOT:PSS exhibit semiconducting behavior [34,35]. The choice of the materials to compose the sensing units was to assist the formation of a "fingerprint" of the soils dispersed in water in the e-tongue analyses; they were not chosen to detect specific macronutrients in the samples.

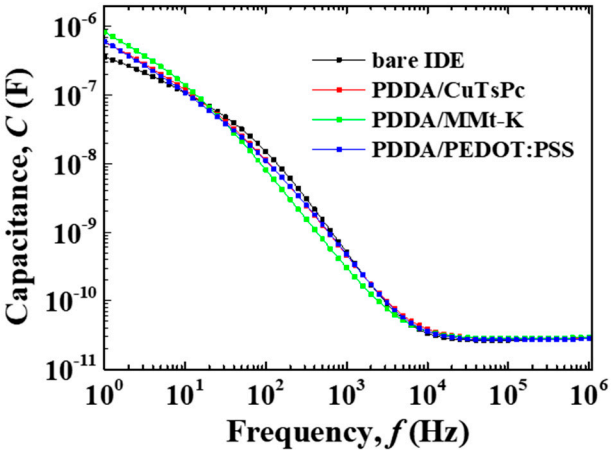

Figure 2. Capacitance spectra for the bare interdigitated electrodes (IDE), PDDA/CuTsPc, PDDA/ montmorillonite clay (MMt-K), and PDDA/ poly(3,4-ethylenedioxythiophene)-poly(styrenesulfonate) (PEDOT:PSS) sensing units in distilled water.

Figure 3 shows three independent measurements of the bare IDE immersed in sandy and clayey soil samples enriched with a higher amount of potassium (S-002, according to the code presented in Table 1). Good reproducibility of the 3D-printed electrode in the evaluation of soil samples can be easily seen, and the same result was observed in three independent measurements for all 4 sensing units in all the 16 soil samples analyzed (Figures S1–S8 in the Supplementary Materials).

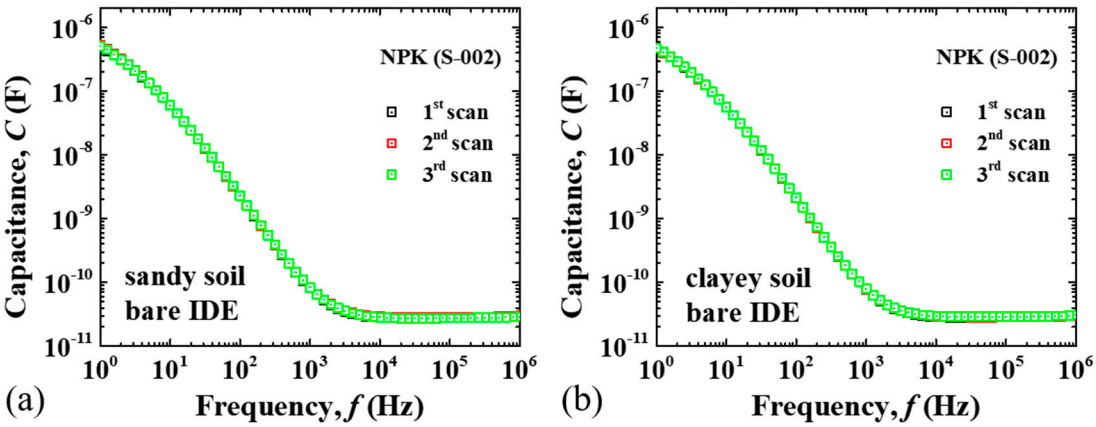

Figure 3. Capacitance versus frequency spectra measured with bare IDE sensing unit for (**a**) sandy and (**b**) clayey soil samples enriched with a higher amount of potassium (S-002) in aqueous solution at 1 mg·mL^{-1}.

Impedance analysis as a function of frequency may allow the identification of potential interactions at the electrode/electrolyte interface through equivalent electrical circuit analysis. More simply, the interactions between the nanostructured thin films forming the sensing units deposited onto the IDEs with the liquid systems are usually reflected in the electrical response at the kilohertz region [36]. Therefore, the fabrication of equipment for on-site developments will be favored for

real-time monitoring by considering measurements only in a single frequency. In this context, Figure 4 presents the PCA plots of the capacitance data at 1 kHz for sandy and clayey soil samples enriched with distinct amounts of N, P, and K (as code presented in Table 1). The use of only two principal components led to 93.5% and 97.5% (PC1 + PC2) of the total information collected by the array for sandy and clayey soils, respectively. Moreover, most information is concentrated in the first principal component (PC1), especially for the clayey soil group (95.4%).

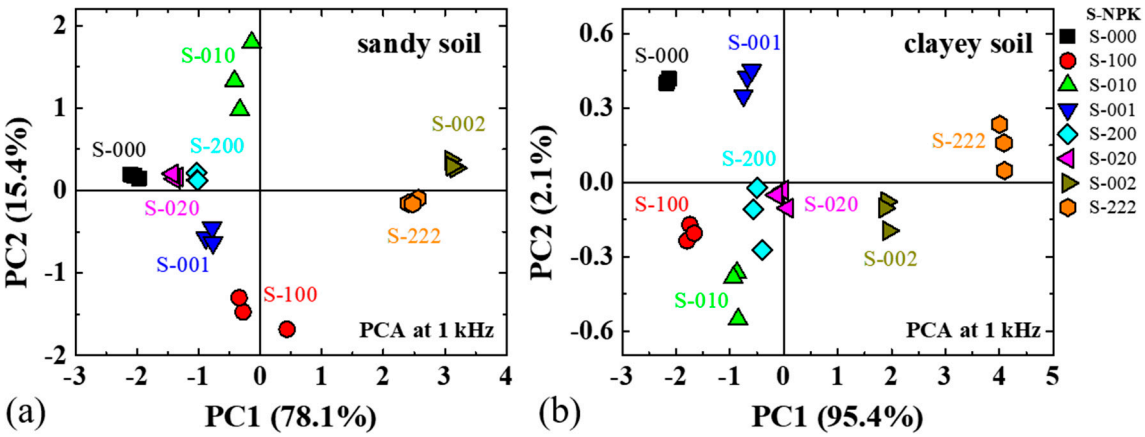

Figure 4. Principal component analysis (PCA) for the 1 kHz capacitance results of the e-tongue system applied to liquid aliquots of (**a**) sandy and (**b**) clayey soil samples enriched with different amounts of N, P and K.

A visual inspection of the PCA plots presented in Figure 4 points to good discrimination of all soil samples, except for samples S-200 and S-020, which did not present considerable distance from each other in both soil groups (sandy (a) and clayey (b)). These samples would probably be considered as a single group in a blind test. From Table 1, the main differences among these samples are the phosphorus content, once potassium was not added (low natural fertility), and the nitrogen amount in S-200 was only slightly higher than in S-020 samples of both soil groups.

In a more general view of the PCA plots, regardless of the soil texture (sandy or clayey), one can see the control samples (000) in the negative outermost x-axes while the S-002 and S-222 samples are found in higher PC1 values. These data suggest that PC1 can be related to soil fertility. The soil samples with the S-222 code are supposed to be those with a higher amount of N, P, and K simultaneously. The S-222 sample of the clayey group (Figure 4b) appears opposite from the control sample (in regards to PC1), while S-002 is on the PC1 positive end for the sandy group (Figure 4a). Based on Table 1, the S-222 sample of the sandy group presented slightly lower amounts of N and K than sample S-002, which could lead to observed changes in position on PC1.

For both soil groups (sandy and clayey), PCA was able to distinguish among soil samples with different content of the same macronutrient. To illustrate, samples with intermediate and high amounts of N (S-100 and S-200), P (S-010 and S-020), and K (S-001 and S-002) were grouped in distinct clusters in the PCA plots (Figure 4). Therefore, from the PCA plots, one can clearly see the system here distinguishes all soil samples not only from distinct macronutrients but also considering samples that have different amounts of the same nutrient.

The analysis for the clayey soil group was replicated within 2 years, and the results (Figure S9 in the Supplementary Information) still presented good reproducibility of the PCA pattern shown in Figure 4b and described above. The idea here is a straightforward time comparison, considering two distinct researchers conducting independent measurements with the same samples and following the same protocol. In addition to good reproducibility, it was also a good indicator of the lifetime of the e-tongue system presented here. The results indicated that PC1 corroborates soil fertility

information in Table 1, with higher changes observed for nitrogen and potassium, and is less sensitive to phosphorous content.

Electrical measurements were also performed in soil samples diluted in distinct concentrations from 0.1 to 1 mg·mL^{-1}, to evaluate the LOD of the 3D printed e-tongue system. To illustrate, Figure 5 shows each point as an average of three capacitance measurements obtained for the bare IDEs sensing unit at 1 kHz from 0.1 to 1 mg·mL^{-1} of sandy and clayey samples enriched with a higher amount of potassium (S-002). Additional data are shown in Figures S10 and S11 in the Supplementary Information. The LOD was calculated similarly to recent literature [37–41] as LOD = (3 × σ)/b, where σ is the standard deviation, and b is the slope of the calibration curve (linear fit).

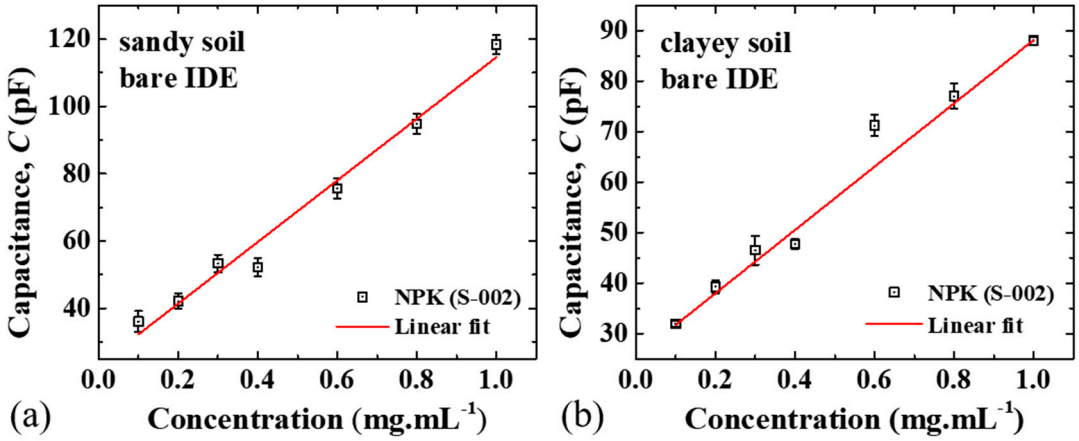

Figure 5. Capacitance data obtained for the bare IDE sensing unit at 1 kHz from 0.1 to 1 mg·mL^{-1} of (**a**) sandy and (**b**) clayey soil samples enriched with a higher amount of potassium (S-002).

Table 2 presents sensitivity and LOD values obtained from the calibration curves and the equation presented above. The analysis was performed on sandy and clayey soils, both of them with control (S-000) and samples enriched with a higher amount of potassium (S-002), using bare IDEs and PDDA/PEDOT:PSS sensing units. Bare IDEs were chosen as it is the common factor among the sensing units (same design and structure), while PDDA/PEDOT:PSS was the sensing unit that presented some deviation on triplicate analysis, a fact that could be related to the sensing unit sensitivity due to the electrical nature of PEDOT:PSS. The control soil samples were used as the standard for comparison; while the S-002 soil samples were chosen for the calibration curves because in the PCA plots, potassium displayed a better trend when compared with the two other macronutrients. Comparing the data from Table 2, the sensitivity of the PDDA/PEDOT:PSS sensing unit is higher than the bare IDE for three out of the four soil samples evaluated. Nevertheless, it is a remarkable result considering the simplicity and time involved in the fabrication process of this e-tongue system using 3D printing technology.

Table 2. Sensitivity and limit of detection (LOD) for bare interdigitated electrodes (IDE) and poly(diallyldimethylammonium chloride) solution/poly(3,4-ethylenedioxythiophene)-poly(styrenesulfonate) (PDDA/PEDOT:PSS) sensing units during soil analysis. The content of this table corresponds to electrical impedance spectroscopy data for the sandy and clayey soil control samples (S-000) and the ones enriched with a higher amount of potassium (S-002).

Sensing Unit	Soil Group	Sample Code (S-NPK)	Sensitivity (pF·mL·mg^{-1})	LOD (mg·mL^{-1})
Bare IDE	sandy	S-000	12 ± 2	0.30 ± 0.04
		S-002	92 ± 6	0.101 ± 0.006
	clayey	S-000	30 ± 5	0.20 ± 0.03
		S-002	63 ± 2	0.065 ± 0.003
PDDA/PEDOT:PSS	sandy	S-000	20 ± 5	0.4 ± 0.1
		S-002	115 ± 7	0.091 ± 0.006
	clayey	S-000	25 ± 1	0.087 ± 0.004
		S-002	70 ± 6	0.14 ± 0.01

4. Conclusions

Good reproducibility and distinction of the sandy and clayey soil samples enriched with N, P, and K were achieved using the e-tongue system based on 3D-printed electrodes. The results were comparable to an e-tongue system based on traditional gold electrodes. However, the electrodes used here were 3D-printed within 20 min. The system was able to distinguish all samples not only from distinct macronutrients but also from samples having distinct amounts of the same nutrient. For both sandy and clayey soils, PCA plots indicated that PC1 can be related to soil fertility, being especially sensitive to N and K content, compared to P.

These are important steps for future developments, including the incorporation of all sensing units in a single platform using the 3D printing technique to integrate the whole system in microfluidic devices (all 3D-printed). With the sensing units used here, we are not able to detect specific macronutrients once we explored the system using the global selectivity concept. However, ongoing studies are being conducted considering the specific detection of at least one macronutrient added in the enrichment of soils (K, for example).

Supplementary Materials: The following are available online at http://www.mdpi.com/2227-9040/7/4/50/s1, Figure S1: Capacitance versus frequency spectra measured with bare IDE sensing unit for sandy soil samples enriched with different amounts of N, P, and K in aqueous solution at 1 mg·mL^{-1}, Figure S2: Capacitance versus frequency spectra measured with PDDA/CuTsPc sensing unit for sandy soil samples enriched with different amounts of N, P, and K in aqueous solution at 1 mg·mL^{-1}, Figure S3: Capacitance versus frequency spectra measured with PDDA/MMt-K sensing unit for sandy soil samples enriched with different amounts of N, P, and K in aqueous solution at 1 mg·mL^{-1}, Figure S4: Capacitance versus frequency spectra measured with PDDA/PEDOT:PSS sensing unit for sandy soil samples enriched with different amounts of N, P, and K in aqueous solution at 1 mg·mL^{-1}, Figure S5: Capacitance versus frequency spectra measured with bare IDE sensing unit for clayey soil samples enriched with different amounts of N, P, and K in aqueous solution at 1 mg·mL^{-1}, Figure S6: Capacitance versus frequency spectra measured with PDDA/CuTsPc sensing unit for clayey soil samples enriched with different amounts of N, P, and K in aqueous solution at 1 mg·mL^{-1}, Figure S7: Capacitance versus frequency spectra measured with PDDA/MMt-K sensing unit for clayey soil samples enriched with different amounts of N, P, and K in aqueous solution at 1 mg·mL^{-1}, Figure S8: Capacitance versus frequency spectra measured with PDDA/PEDOT:PSS sensing unit for clayey soil samples enriched with different amounts of N, P, and K in aqueous solution at 1 mg·mL^{-1}, Figure S9: Principal component analysis (PCA) for the 1 kHz capacitance data of the e-tongue system applied to liquid aliquots of clayey soil samples enriched with different amounts of N, P and K. These data were obtained ~2 years before the results presented in the manuscript. Both experiments followed the same procedure, with new sensing units fabricated for the distinct tests, Figure S10: Capacitance data obtained for the bare IDE sensing unit at 1 kHz of sandy and clayey soil control samples and enriched with a higher amount of potassium (S-002), Figure S11: Capacitance data obtained for the PDDA/PEDOT:PSS sensing unit at 1 kHz of sandy and clayey soil control samples and enriched with a higher amount of potassium (S-002).

Author Contributions: Conceptualization, M.L.B. and A.R.J.; methodology, A.R.J.; validation, T.A.d.S. and M.L.B.; formal analysis, T.A.d.S. and M.L.B.; investigation, T.A.d.S.; resources, M.A.N.C., L.R.d.A., V.R. and A.R.J.; data curation, T.A.d.S.; writing—original draft preparation, T.A.d.S. and M.L.B.; writing—review and editing, M.A.N.C., L.R.d.A., V.R. and A.R.J.; visualization, T.A.d.S. and M.L.B.; supervision, A.R.J.; project administration, A.R.J.; funding acquisition, M.L.B., L.R.d.A., V.R. and A.R.J.

Funding: This research was funded by the Brazilian agencies: São Paulo Research Foundation (FAPESP, grant number 2015/14836-9 and 2015/21616-5), the Coordenação de Aperfeiçoamento de Pessoal de Nível Superior (CAPES) and the National Council for Scientific and Technological Development (CNPq).

Conflicts of Interest: The authors declare no conflict of interest.

References

1. Crist, E.; Mora, C.; Engelman, R. The interaction of human population, food production, and biodiversity protection. *Science* **2017**, *356*, 260–264. [CrossRef]
2. Mishra, P.; Mapara, S.; Vyas, P. Testing/monitoring of soil chemical level using wireless sensor network technology. *Int. J. Appl. Innov. Eng. Manag.* **2015**, *4*, 114–117.
3. Rogovska, N.; Laird, D.A.; Chiou, C.-P.; Bond, L.J. Development of field mobile soil nitrate sensor technology to facilitate precision fertilizer management. *Precis. Agric.* **2019**, *20*, 40–55. [CrossRef]
4. De Camargo, O.A.; Moniz, A.C.; Jorge, J.A.; Valadares, J.M.A.S. *Methods of Chemical, Mineralogical and Physical Analysis of Soils of the Agronomic Institute of Campinas*, 2nd ed.; Instituto Agronomico de Campinas: Campinas, Brazil, 2009.
5. Cherubin, M.R.; Santi, A.L.; Eitelwein, M.T.; Menegol, D.R.; Da Ros, C.O.; de Castro Pias, O.H.; Berghetti, J. Efficiency of sampling grids used in the characterization of phosphorus and potassium. Ciência. *Rural* **2014**, *44*, 425–432. [CrossRef]
6. Nanni, M.R.; Povh, F.P.; Demattê, J.A.M.; de Oliveira, R.B.; Chicati, M.L.; Cezar, E. Optimum size in grid soil sampling for variable rate application in site-specific management. *Sci. Agric.* **2011**, *68*, 386–392. [CrossRef]
7. Viscarra Rossel, R.A.; McBratney, A.B.; Minasny, B. (Eds.) *Proximal Soil Sensing*; Springer Netherlands: Heidelberg, Germany, 2010; ISBN 9789048188581.
8. Podrazka, M.; Baczynska, E.; Kundys, M.; Jelen, P.S.; Nery, E.W. Electronic tongue—A tool for all tastes? *Biosensors* **2018**, *8*, 3. [CrossRef]
9. Toko, K. Taste sensor with global selectivity. *Mater. Sci. Eng. C* **1996**, *4*, 69–82. [CrossRef]
10. Legin, A.; Rudnitskaya, A.; Vlasov, Y.; Di Natale, C.; Davide, F.; D'Amico, A. Tasting of beverages using an electronic tongue. *Sens. Actuators B Chem.* **1997**, *44*, 291–296. [CrossRef]
11. Di Natale, C.; Macagnano, A.; Davide, F.; D'Amico, A.; Legin, A.; Vlasov, Y.; Rudnitskaya, A.; Selezenev, B. Multicomponent analysis on polluted waters by means of an electronic tongue. *Sens. Actuators B Chem.* **1997**, *44*, 423–428. [CrossRef]
12. Daikuzono, C.M.; Shimizu, F.M.; Manzoli, A.; Riul, A.; Piazzetta, M.H.O.; Gobbi, A.L.; Correa, D.S.; Paulovich, F.V.; Oliveira, O.N. Information visualization and feature selection methods applied to detect gliadin in gluten-containing foodstuff with a microfluidic electronic tongue. *ACS Appl. Mater. Interfaces* **2017**, *9*, 19646–19652. [CrossRef]
13. Carbó, N.; López Carrero, J.; Garcia-Castillo, F.; Tormos, I.; Olivas, E.; Folch, E.; Alcañiz Fillol, M.; Soto, J.; Martínez-Máñez, R.; Martínez-Bisbal, M. Quantitative determination of spring water quality parameters via electronic tongue. *Sensors* **2018**, *18*, 40. [CrossRef]
14. Salvo-Comino, C.; García-Hernández, C.; García-Cabezón, C.; Rodríguez-Méndez, M.L. Discrimination of milks with a multisensor system based on layer-by-layer films. *Sensors* **2018**, *18*, 2716. [CrossRef]
15. Daikuzono, C.M.; Delaney, C.; Morrin, A.; Diamond, D.; Florea, L.; Oliveira, O.N. Paper based electronic tongue-a low-cost solution for the distinction of sugar type and apple juice brand. *Analyst* **2019**, *144*, 2827–2832. [CrossRef]
16. De Morais, T.C.B.; Rodrigues, D.R.; de Carvalho Polari Souto, U.T.; Lemos, S.G. A simple voltammetric electronic tongue for the analysis of coffee adulterations. *Food Chem.* **2019**, *273*, 31–38. [CrossRef]
17. Lvova, L.; Guanais Gonçalves, C.; Petropoulos, K.; Micheli, L.; Volpe, G.; Kirsanov, D.; Legin, A.; Viaggiu, E.; Congestri, R.; Guzzella, L.; et al. Electronic tongue for microcystin screening in waters. *Biosens. Bioelectron.* **2016**, *80*, 154–160. [CrossRef]

18. Ferreira, N.S.; Cruz, M.G.N.; Gomes, M.T.S.R.; Rudnitskaya, A. Potentiometric chemical sensors for the detection of paralytic shellfish toxins. *Talanta* **2018**, *181*, 380–384. [CrossRef]
19. Shimizu, F.M.; Braunger, M.L.; Riul, A., Jr. Heavy metal/toxins detection using electronic tongues. *Chemosensors* **2019**, *7*, 36. [CrossRef]
20. Facure, M.H.M.; Mercante, L.A.; Mattoso, L.H.C.; Correa, D.S. Detection of trace levels of organophosphate pesticides using an electronic tongue based on graphene hybrid nanocomposites. *Talanta* **2017**, *167*, 59–66. [CrossRef]
21. Qiao, L.; Qian, S.; Wang, Y.; Lin, H. A colorimetric sensor array based on sulfuric acid assisted $KMnO_4$ fading for the detection and identification of pesticides. *Talanta* **2018**, *181*, 305–310. [CrossRef]
22. Wang, F.; Zhang, X.; Lu, Y.; Yang, J.; Jing, W.; Zhang, S.; Liu, Y. Continuously evolving 'chemical tongue' biosensor for detecting proteins. *Talanta* **2017**, *165*, 182–187. [CrossRef]
23. Saidi, T.; Moufid, M.; Zaim, O.; El Bari, N.; Bouchikhi, B. Voltammetric electronic tongue combined with chemometric techniques for direct identification of creatinine level in human urine. *Meas. J. Int. Meas. Confed.* **2018**, *115*, 178–184. [CrossRef]
24. Solovieva, S.; Karnaukh, M.; Panchuk, V.; Andreev, E.; Kartsova, L.; Bessonova, E.; Legin, A.; Wang, P.; Wan, H.; Jahatspanian, I.; et al. Potentiometric multisensor system as a possible simple tool for non-invasive prostate cancer diagnostics through urine analysis. *Sens. Actuators B Chem.* **2019**, *289*, 42–47. [CrossRef]
25. Mimendia, A.; Gutiérrez, J.M.; Alcañiz, J.M.; del Valle, M. Discrimination of soils and assessment of soil fertility using information from an ion selective electrodes array and artificial neural networks. *Clean Soil Air Water* **2014**, *42*, 1808–1815. [CrossRef]
26. Braunger, M.L.; Shimizu, F.M.; Jimenez, M.J.M.; Amaral, L.R.; de Oliveira Piazzetta, M.H.; Gobbi, Â.L.; Magalhães, P.S.G.; Rodrigues, V.; Oliveira, O.N., Jr.; Riul, A., Jr. Microfluidic electronic tongue applied to soil analysis. *Chemosensors* **2017**, *5*, 14. [CrossRef]
27. Cummins, G.; Desmulliez, M.P.Y. Inkjet printing of conductive materials: A review. *Circuit World* **2012**, *38*, 193–213. [CrossRef]
28. Paula, K.T.; Gaál, G.; Almeida, G.F.B.; Andrade, M.B.; Facure, M.H.M.; Correa, D.S.; Riul, A.; Rodrigues, V.; Mendonça, C.R. Femtosecond laser micromachining of polylactic acid/graphene composites for designing interdigitated microelectrodes for sensor applications. *Opt. Laser Technol.* **2018**, *101*, 74–79. [CrossRef]
29. Xu, Y.; Wu, X.; Guo, X.; Kong, B.; Zhang, M.; Qian, X.; Mi, S.; Sun, W. The Boom in 3D-Printed Sensor Technology. *Sensors* **2017**, *17*, 1166. [CrossRef]
30. Gaál, G.; Silva, T.A.; Gaál, V.; Hensel, R.C.; Amaral, L.R.; Rodrigues, V.; Riul, A., Jr. 3D Printed e-tongue. *Front. Chem.* **2018**, *6*, 1–8. [CrossRef]
31. Decher, G. Fuzzy nanoassemblies: Toward layered polymeric multicomposites. *Science* **1997**, *277*, 1232–1237. [CrossRef]
32. Coutinho, M.A.N.; Alari, F.d.O.; Ferreira, M.M.C.; Amaral, L.R.d. Influence of soil sample preparation on the quantification of NPK content via spectroscopy. *Geoderma* **2019**, *338*, 401–409. [CrossRef]
33. Kato, C.; Kuroda, K.; Takahara, H. Preparation and electrical properties of quaternary ammonium montmorillonite-polystyrene complexes. *Clays Clay Miner.* **1981**, *29*, 294–298. [CrossRef]
34. Bao, Z.; Lovinger, A.J.; Dodabalapur, A. Organic field-effect transistors with high mobility based on copper phthalocyanine. *Appl. Phys. Lett.* **1996**, *69*, 3066–3068. [CrossRef]
35. Nardes, A.M.; Kemerink, M.; Janssen, R.A.J.; Bastiaansen, J.A.M.; Kiggen, N.M.M.; Langeveld, B.M.W.; van Breemen, A.J.J.M.; de Kok, M.M. Microscopic understanding of the anisotropic conductivity of PEDOT: PSS thin films. *Adv. Mater.* **2007**, *19*, 1196–1200. [CrossRef]
36. Riul, A., Jr.; dos Santos, D.S., Jr.; Wohnrath, K.; Di Tommazo, R.; Carvalho, A.C.P.L.F.; Fonseca, F.J.; Oliveira, O.N., Jr.; Taylor, D.M.; Mattoso, L.H.C. Artificial taste sensor: Efficient combination of sensors made from Langmuir-Blodgett films of conducting polymers and a ruthenium complex and self-assembled films of an azobenzene-containing polymer. *Langmuir* **2002**, *18*, 239–245. [CrossRef]
37. De Barros, A.; Constantino, C.J.L.; da Cruz, N.C.; Bortoleto, J.R.R.; Ferreira, M. High performance of electrochemical sensors based on LbL films of gold nanoparticles, polyaniline and sodium montmorillonite clay mineral for simultaneous detection of metal ions. *Electrochim. Acta* **2017**, *235*, 700–708. [CrossRef]
38. Kang, W.; Pei, X.; Rusinek, C.A.; Bange, A.; Haynes, E.N.; Heineman, W.R.; Papautsky, I. Determination of lead with a copper-based electrochemical sensor. *Anal. Chem.* **2017**, *89*, 3345–3352. [CrossRef]

39. De Lucena, N.C.; Miyazaki, C.M.; Shimizu, F.M.; Constantino, C.J.L.; Ferreira, M. Layer-by-layer composite film of nickel phthalocyanine and montmorillonite clay for synergistic effect on electrochemical detection of dopamine. *Appl. Surf. Sci.* **2018**, *436*, 957–966. [CrossRef]
40. Rodrigues, G.H.S.; Miyazaki, C.M.; Rubira, R.J.G.; Constantino, C.J.L.; Ferreira, M. Layer-by-layer films of graphene nanoplatelets and gold nanoparticles for methyl parathion sensing. *ACS Appl. Nano Mater.* **2019**, *2*, 1082–1091. [CrossRef]
41. Camilo, D.E.; Miyazaki, C.M.; Shimizu, F.M.; Ferreira, M. Improving direct immunoassay response by layer-by-layer films of gold nanoparticles—Antibody conjugate towards label-free detection. *Mater. Sci. Eng. C* **2019**, *102*, 315–323. [CrossRef]

© 2019 by the authors. Licensee MDPI, Basel, Switzerland. This article is an open access article distributed under the terms and conditions of the Creative Commons Attribution (CC BY) license (http://creativecommons.org/licenses/by/4.0/).